

Efimov-driven phase transitions of the unitary Bose gas

Swann Piatecki¹ & Werner Krauth¹

¹*Laboratoire de Physique Statistique, École Normale Supérieure, UPMC, Université Paris Diderot, CNRS, 24 rue Lhomond, 75005 Paris, France*

In quantum physics, Efimov trimers¹⁻³ are bound states of three particles that fall apart like Borromean rings when one of them is removed. Initially predicted in nuclear physics, these striking bosonic states are hard to observe, but the “unitary” interactions at which they form is commonly realized in current cold atoms experiments⁴⁻⁷. There, they set the stage for a new class of universal physics: Two-body interactions are all but invisible, but three-body effects allow the emergence of a largely uncharted new world of many-particle bound states. Three-particle systems were characterized theoretically⁸, and the ground-state properties of small unitary clusters computed numerically⁹, but the macroscopic many-body behaviour has remained unknown. Here we show, using a Path-Integral Monte Carlo algorithm¹⁰⁻¹² backed up by theoretical arguments, that the unitary Bose gas presents a first-order phase transition from a normal gas to a superfluid Efimov liquid. The normal gas is very well described by the available virial coefficients¹³. At unitarity, the phase diagram of the bosonic system is universal in rescaled pressure and temperature. A triple point separates the normal gas, the superfluid Efimov liquid, and a third phase, the conventional superfluid gas. These two superfluid phases are separated by a critical line that ends in a critical point at high temperature. This rich phase diagram should allow for a number of experimental protocols

that would probe these universal transitions between the normal gas, the superfluid gas, and the superfluid Efimov liquid.

We describe the system of N interacting bosons by a hamiltonian

$$H = \sum_i \frac{\mathbf{p}_i^2}{2m} + \sum_{i<j} V_2^a(r_{ij}) + \sum_{i<j<k} V_3(R_{ijk}) + \frac{m\omega^2}{2} \sum_i \mathbf{x}_i^2, \quad (1)$$

where \mathbf{p}_i , \mathbf{x}_i and m are the momentum, the position and the mass of particle i . The pair interaction V_2^a is of range zero, and its unitary point corresponds to an infinite scattering length a . The three-body interaction V_3 implements a hard-core hyperradial cutoff condition, $R_{ijk} > R_0$, where the hyperradius R_{ijk} of particles i , j , and k corresponds to their root-mean-square pair distance ($3R_{ijk}^2 = r_{ij}^2 + r_{ik}^2 + r_{jk}^2$). This three-body hard core prevents the so-called Thomas collapse¹⁴ into a many-body state with vanishing extension and infinite negative energy by setting a fundamental trimer energy $-E_t \propto R_0^{-2}$. The final term in Eq. (1) models an isotropic harmonic trapping potential of length $a_\omega = \sqrt{\hbar/(m\omega)}$ as it is realised in ultracold bosons experiments (see Supplementary Discussion 1 for a full description of the hamiltonian). The properties of the system described by Eq. (1) are universal when R_0 is much smaller than all other length scales. Unlike the hamiltonian of Eq. (1), experimental systems of cold atoms tuned to unitarity at a Feshbach resonance¹⁵ are metastable because of the presence of deeply bound states. When three particles get too close, they leave the trap and contribute to the notorious three-body losses. In experiments, the three-body parameter given by R_0 depends on pair interaction parameters specific to each atomic species¹⁶.

In thermal equilibrium, within the path-integral representation of quantum systems that we use for our computations, position variables $\mathbf{x}_i(\tau)$ carry an imaginary-time index $\tau \in [0, \beta =$

$1/k_B T]$, where k_B is the Boltzmann constant. The fluctuations of $\mathbf{x}_i(\tau)$ along τ account for the quantum uncertainty. The bosonic nature of many-particle systems manifests itself through the periodic boundary conditions in τ and, in particular, through the permutation structure of particles. The length of permutation cycles correlates with the degree of quantum coherence^{17,18}. Interactions set the statistical weights of configurations¹⁰. Ensemble averaging, performed by a dedicated Quantum Monte Carlo algorithm, yields the complete thermodynamics of the system (see Supplementary Discussion 2 for computational details). The N -body simulation code is massively run on a cluster of independent processors. It succeeds in equilibrating samples with up to a few hundred bosons.

Snapshots for three particles in a shallow trap at $\omega \sim 0$ illustrate the quantum fluctuations in $\mathbf{x}_i(\tau)$, and characterize the Efimov trimer. Indeed, for two-body interactions without a bound state, virtually free particles fluctuate on the scale of the de Broglie wavelength $\lambda_{\text{th}} = \sqrt{2\pi\hbar^2\beta/m}$ that diverges at low temperature (see Fig. 1a). In contrast, for positive a , a bound state with energy $-E_{\text{dimer}} = -\hbar^2/(ma^2)$ forms in the two-body interaction potential. Two particles bind into a dimer, and the third particle is free (see Fig. 1c). Efimov physics takes place at unitarity, where the bound state of the pair potential is at resonance $E_{\text{dimer}} = 0$, and the scattering length a is infinite (see Fig. 1b)). At this point, the two-body interaction is scale-free. While two isolated particles do not bind, in the three-particle system, pairs of particles approach each other, and then dissociate, so that, between $\tau = 0$ and $\tau = \beta$, the identity of close-by partners changes several times. This coherent particle-pair scattering process, the hallmark of the Efimov effect³, is highlighted in Fig. 1b. At small temperatures, the fluctuations of this bound state remain on a scale proportional to R_0 and

do not diverge as λ_{th} . We obtain excellent agreement of the probability distribution of the hyperradius R with its analytically known distribution $p_R(R)$ (see Fig. 1d). This effectively validates our algorithm. Furthermore, the observed quadratic divergence of the pair distance distribution $\rho_r(r)$, leading to an asymptotically constant $r^2\rho_r(r)$ for $r \rightarrow 0$, checks with the Bethe–Peierls condition for the zero-range unitary potential¹⁹ (see Supplementary Discussion 1).

In local-density approximation, particles experience an effective chemical potential $\mu(r) = \mu_0 - m\omega^2 r^2/2$ that depends on the distance r to the centre of the trap. This allows us²⁰ to obtain the grand-canonical equation of state (pressure P as a function of μ) from the configurations of a single simulation run at temperature T . We find that the equation of state is described very accurately by the virial expansion up to third order in the fugacity $e^{\beta\mu}$ (see Fig. 2 and Supplementary Discussion 4)¹³. The third-order term is crucial to the description of Efimov physics as it is the first term at which three-body effects appear²¹. It depends explicitly on T and R_0 .

In the harmonic trap, particles can be in different thermodynamic phases depending on the distance r from its centre. We monitor the correlation between the pair distances and the position in the trap, and are able to track the creation of a drop of high-density liquid at $r \sim 0$ (see Fig. 3a-c). This drop grows as the temperature decreases. The observed behaviour corresponds to a first-order normal-gas-to-superfluid-liquid transition. All particles in the drop are linked through coherent close-by particle switches as in Fig. 1b, showing that the drop is superfluid. Deep inside the liquid phase, the Quantum Monte Carlo simulation drops out of equilibrium on the available simulation times. Nevertheless, at its onset and throughout the values of R_0 , the peak of the pair correlation

function is located around $10R_0$, which indicates that the liquid phase is of constant density $n_l \propto R_0^{-3}$ (see Fig. 3c). At larger values of R_0 , the density difference between the trap centre and the outside vanishes continuously, and the phase transition is no longer seen (see Fig. 3d-f). Beyond this critical point, the peak of the pair correlation also stabilizes around $10R_0$, which indicates a crossover to liquid behaviour (see Fig. 3f and Supplementary Discussion 5 for additional details on the characterization of the first-order phase transition).

Our numerical findings suggest a theoretical model for the competition between the unitary gas in third-order virial expansion and an incompressible liquid of density $n_l \propto R_0^{-3}$ and constant energy per particle $-\epsilon \propto E_t$, as suggested by ground-state computations for small clusters⁹. For simplicity, we neglect the entropic contributions to the liquid-state free energy $\epsilon \gg TS$, so that $F_{\text{liquid}} \approx -N\epsilon$. The phase equilibrium is due to the difference in free energy and in specific volume at the saturated vapour pressure (see Supplementary Discussion 6). We extend the third-order virial expansion to describe the gaseous phase in the region where quantum correlations become important. Because the conventional superfluid transition is continuous, it still conveys qualitative information about the transition into the superfluid Efimov liquid in that region. At small $R_0 \rightarrow 0$, the coexistence line approaches infinite temperatures, as the fundamental trimer energy $E_t \propto R_0^{-2}$ diverges. For larger values of R_0 , the density of the liquid decreases and approaches the one of the gas. The liquid–gas transition line ends in a critical point, where both densities coincide. As the liquid is bound by quantum coherence intrinsic to the Efimov effect, this critical point must always be inside a superfluid. The agreement between this approximate theory and numerical calculations for the trap centre phase diagram is remarkable (see Fig. 4a). Beyond the critical point, we no

longer observe a steep drop in the density on decreasing the temperature. We also notice that quantum coherence builds up in the gaseous phase, so that only a conventional superfluid transition takes place. Our numerical results suggests it occurs at a temperature slightly lower than that for the ideal Bose gas²², $T_{\text{BEC}}^0 \approx \hbar\omega(0.94N^{1/3} - 0.69)$.

Our theoretical model also yields a phase diagram for a homogeneous system of unitary bosons (see Fig. 4b), where, in addition, the conventional superfluid transition is simply modelled by that of free bosons²³. In absence of a harmonic trap, only two independent dimensionless numbers may be built, $k_B T/\epsilon$, and $P\hbar^3/\sqrt{m^3\epsilon^5}$. As a consequence, the phase diagram in these two dimensionless numbers is independent of the choice of ϵ , that is, of R_0 . The scalings of the rescaled pressure with R_0^5 and of the rescaled temperature with R_0^2 , explain that the triple point appears much farther from the critical point in the homogeneous phase diagram than in the trap. We expect model-dependent non-universal effects in two regions. At high temperature $\lambda_{\text{th}} \ll R_0$, only a classical gas should exist as the hyperradial cutoff is much smaller than the de Broglie thermal wavelength, and therefore prevents the build-up of quantum coherence. At high pressure $P \propto T$, we expect a classical solid phase driven by entropic effect, as for conventional hard-sphere melting.

In present-day cold atom experiments, unitarity is achieved by tuning the scattering length to infinity using Feshbach resonances¹⁵. In experimental systems, the observation of thermodynamic states of the unitary Bose gas is rendered difficult by the same three-body losses although, on the other hand, these losses serve to characterize Efimov trimers⁴⁻⁶. Notwithstanding these complica-

tions, for long-lived systems where the recombination rate into non-universal deeply bound states is sufficiently small⁷, it should be possible to measure the virial corrections to the equation of state and to probe the universal phase diagram.

Acknowledgements

We thank S. Balibar, Y. Castin, F. Chevy, B. Rem, C. Salomon, and F. Werner for very helpful discussions. W.K. acknowledges the hospitality of the Aspen Center for Physics, which is supported by the National Science Foundation Grant No. PHY-1066293.

1. Efimov, V. Energy levels arising from resonant two-body forces in a three-body system. *Phys. Lett. B* **33**, 563–564 (1970).
2. Efimov, V. Weakly-bound states of three resonantly-interacting particles. *Sov. J. Nucl. Phys.* **12**, 589–595 (1971).
3. Efimov, V. Low-energy property of three resonantly interacting particles. *Sov. J. of Nucl. Phys.* **29**, 1058–1069 (1979).
4. Gross, N., Shotan, Z., Kokkelmans, S. & Khaykovich, L. Observation of universality in ultracold ⁷Li three-body recombination. *Phys. Rev. Lett.* **103**, 163202 (2009).
5. Pollack, S. E., Dries, D. & Hulet, R. G. Universality in three- and four-body bound states of ultracold atoms. *Science* **326**, 1683–1685 (2009). PMID: 19965389.

6. Zaccanti, M. *et al.* Observation of an Efimov spectrum in an atomic system. *Nature Phys.* **5**, 586–591 (2009).
7. Rem, B. S. *et al.* Lifetime of the bose gas with resonant interactions. *Phys. Rev. Lett.* **110**, 163202 (2013).
8. Braaten, E. & Hammer, H.-W. Universality in few-body systems with large scattering length. *Phys. Rep.* **428**, 259–390 (2006).
9. von Stecher, J. Weakly bound cluster states of Efimov character. *J. Phys. B* **43**, 101002 (2010).
10. Pollock, E. L. & Ceperley, D. M. Simulation of quantum many-body systems by path-integral methods. *Phys. Rev. B* **30**, 2555–2568 (1984).
11. Krauth, W. Quantum Monte Carlo calculations for a large number of bosons in a harmonic trap. *Phys. Rev. Lett.* **77**, 3695–3699 (1996).
12. Navon, N. *et al.* Dynamics and thermodynamics of the low-temperature strongly interacting Bose gas. *Phys. Rev. Lett.* **107**, 135301 (2011).
13. Castin, Y. & Werner, F. Le troisième coefficient du viriel du gaz de bose unitaire. *Canad. J. Phys.* **91**, 382–389 (2013). [arxiv:1212/5512\(Englishversion\)](#).
14. Thomas, L. H. The interaction between a neutron and a proton and the structure of h^3 . *Phys. Rev.* **47**, 903–909 (1935).
15. Chin, C., Grimm, R., Julienne, P. & Tiesinga, E. Feshbach resonances in ultracold gases. *Rev. Mod. Phys.* **82**, 1225–1286 (2010).

16. Ferlaino, F. *et al.* Efimov resonances in ultracold quantum gases. *Few-Body Systems* **51**, 113–133 (2011).
17. Feynman, R. P. *Statistical mechanics: A set of lectures* (Addison-Wesley, 1982).
18. Krauth, W. *Statistical Mechanics: Algorithms and Computations* (Oxford University Press, Oxford, Great Britain, 2006).
19. Bethe, H. A. & Peierls, R. The scattering of neutrons by protons. *Proc. R. Soc. Lond., A* **149**, 176–183 (1935).
20. Ho, T.-L. & Zhou, Q. Obtaining the phase diagram and thermodynamic quantities of bulk systems from the densities of trapped gases. *Nature Phys.* **6**, 131–134 (2010).
21. Huang, K. *Statistical mechanics* (Wiley, New York, 1987), 2nd edn.
22. Dalfovo, F., Giorgini, S., Pitaevskii, L. P. & Stringari, S. Theory of Bose-Einstein condensation in trapped gases. *Rev. of Mod. Phys.* **71**, 463–512 (1999).
23. Landau, L. D. & Lifshitz, L. M. *Statistical physics*. No. 5 in Course of theoretical physics (Butterworth-Heinemann, 1980), 3rd edn.

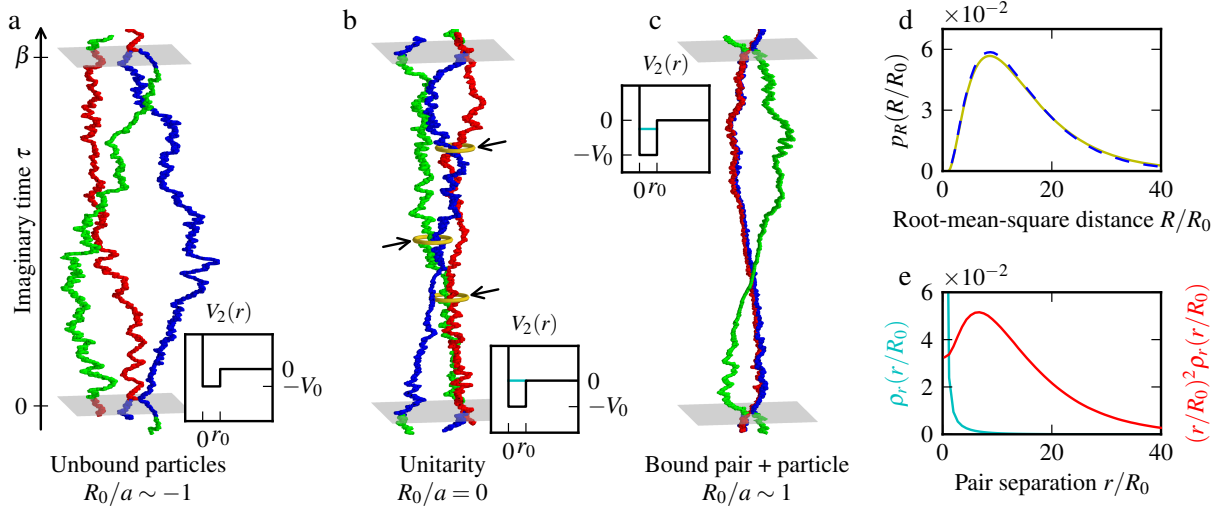


Figure 1: **Path-integral representation of three bosons at different scattering lengths** at $R_0/\lambda_{\text{th}} = 1.3 \times 10^{-2}$ (for the graphical projection of (x, y, z, τ) to three dimensions, see Supplementary Discussion 3). **a.** At $R_0/a \sim -1$, bosons are unbound and fluctuate on a scale λ_{th} . **b.** At unitarity ($R_0/a = 0$), pairs of bosons form and break up throughout the imaginary time (yellow highlights, arrows), forming a three-body state bound by pair effects. **c.** At $R_0/a \sim 1$, two bosons bind into a stable dimer (*red, blue*) and one boson is unbound (*green*). Insets in **a-c** correspond to finite-range versions of the zero-range interaction used in each case. Blue levels correspond to the dimer energy. **d.** Sample-averaged hyperradial (root-mean-square pair distance) probability $p_R(R)$ at constant τ (*solid yellow*) compared to its analytic zero-temperature value⁸ (*dashed blue*). **e.** Sample-averaged pair distribution $\rho_r(r)$, diverging $\propto 1/r^2$ as $r \rightarrow 0$, and asymptotically constant r -shell probability $r^2 \rho_r(r)$, in agreement with the Bethe–Peierls condition. Data in this figure concern co-cyclic particles in a shallow trap of $\omega \sim 0$ (see Supplementary Discussion 3).

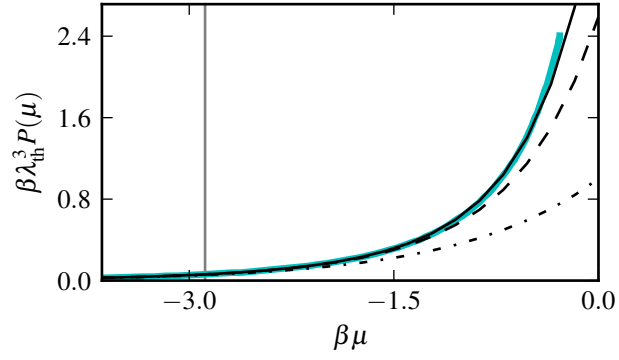


Figure 2: **Equation of state of unitary bosons in a harmonic trap** at $R_0/a_\omega = 0.18$ and $k_B T/\hbar\omega = 38.5$ and $N = 100$. The numerical equation of state for $N = 100$ (*solid cyan line*) obtained by ensemble averaging of configurations²⁰ is compared to the theoretical virial expansion up to the 1st (*dash-dotted black line*), 2nd (*dashed black line*), and 3rd (*solid black line*) virial coefficients. The vertical gray line indicates the most central region of the trap used to determine μ_0 by comparison to an ideal gas.

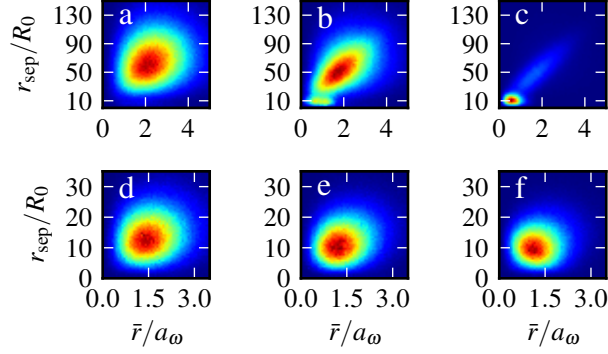


Figure 3: **Two-dimensional histogram of pair distances r_{sep} and centre-of-mass positions \bar{r} .**

Upper panels: *First-order phase transition for $R_0/a_\omega = 0.07$.* **a.** At $k_B T/\hbar\omega = 6.25$, the distribution is that of the normal phase. **b.** At a slightly lower temperature $k_B T/\hbar\omega = 5.88$, a second peak with smaller pair distances $\sim 10R_0$ appears in the trap centre. **c.** At $k_B T/\hbar\omega = 5.56$, most particles are in the trap centre, with small pair distances $\sim 10R_0$. **Lower panels:** *Smooth dependence of pair distances and densities on temperature.* At $R_0/a_\omega = 0.23$, the pair distances decrease smoothly between $k_B T/\hbar\omega = 3.33$ (**d**) and $k_B T/\hbar\omega = 2.94$ (**e**) and has stabilized around $10R_0$ at $k_B T/\hbar\omega = 2.63$ (**f**).

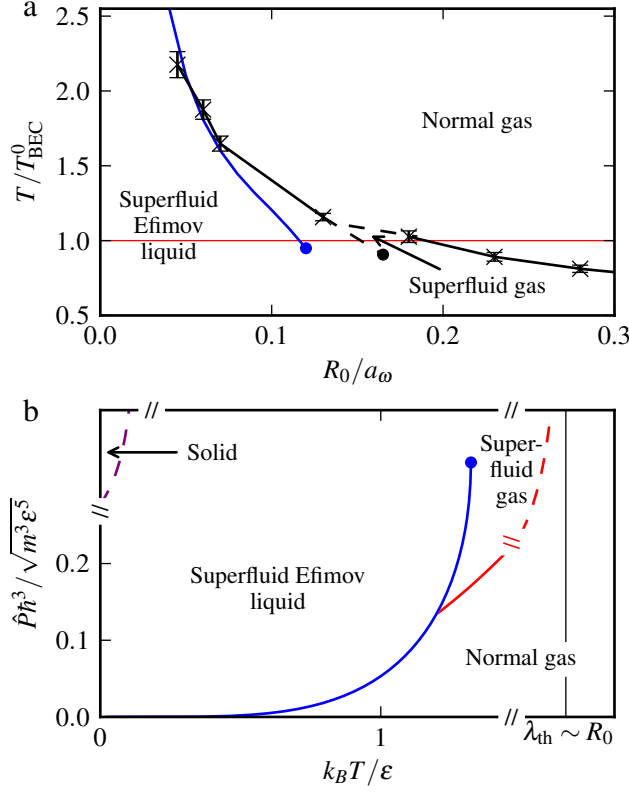


Figure 4: **Phase diagram of the unitary bosons in the trap centre and in homogeneous space.**

a. In the harmonic trap, depending on the value of R_0/a_ω , we observe a normal-gas-to-superfluid-liquid first order phase transition or a conventional second-order superfluid phase transition (*solid, black lines*). The normal-gas-to-superfluid-liquid phase transition corresponds well to our theoretical model (*solid, blue line*) at high temperatures. Consistently with theoretical predictions, the numerical coexistence lines are qualitatively continued to a triple point and a critical point (*dashed black and dashed green lines*). **b.** In a homogeneous system, the normal-gas-to-superfluid-liquid coexistence line (*solid, blue*) and the conventional superfluid transition line (*solid, red*) are universal. The predicted divergence of the normal-gas-to-superfluid-liquid coexistence line (*dashed, red*) and the phase transition to a solid phase (*dashed, purple*) are non-universal physics specific to our interaction model.